

GEOLOGIC CONTEXT OF LACUSTRINE MINERAL DEPOSITS AT BRADBURY CRATER, MARS.

D. Tirsch¹, G. Erkeling², J. L. Bishop³, L. L. Tornabene⁴, H. Hiesinger² and R. Jaumann^{1,5} ¹Institute of Planetary Research, German Aerospace Center (DLR), Berlin, Germany (daniela.tirsch@dlr.de). ²Institut für Planetologie, Westfälische Wilhelms-Universität Münster, Germany. ³Carl Sagan Center, SETI Institute, Mountain View, CA, USA. ⁴Dept. of Earth Sciences, Centre for Planetary Science and Exploration, University of Western Ontario, London, Canada. ⁵Institute of Geological Sciences, Freie Universität Berlin, Berlin, Germany.

Introduction: The 60-km Bradbury Crater (85.8°E; 2.7°N) is located at the Libya Montes region at the southern rim of the Isidis impact basin on Mars. This area is predominantly characterized by Noachian-aged highland massifs that were heavily modified by fluvial, lacustrine, aeolian, volcanic, and impact processes occurring in multiple recurring events [e.g., 1-7]. Bradbury Crater stands out for its abundance of fluvial and lacustrine landforms, which reflect a varied history of aqueous-related geological processes [5,8]. A 2.8 by 5 km-sized fan-shaped deposit has been interpreted to have played a significant role in the hydrologic evolution of landforms at Bradbury Crater [8] (Fig. 1). This deposit is partly composed of Al-rich phyllosilicates, indicating aqueous alteration processes. Current work is directed towards shedding light on the origin and timing of these aqueous alteration processes. It is part of a coordinated analysis of the geological history of Bradbury Crater [cf., 8] and the wider central Libya Montes area [6, and papers in prep.].

Methods: Geological analyses have been performed on the basis of CTX and HiRISE image data in combination with HRSC and HiRISE digital elevation models. Mineral detection has been performed by spectral analyses of targeted CRISM images. Spectral images are processed for instrumental effects, converted to I/F and atmospheric components are minimized using a ratio with a CRISM scene of Olympus Mons [9]. Ratios to spectrally neutral regions in the same column are employed to emphasize spectral absorption features due to distinctive minerals. Spectral parameter maps [9] were used to map trends in the mineralogy and to visualize the mineral locations. Geologic profiles have been created in ESRI's ArcMap tool using HRSC DTMs as the fundamental topographic database.

Observations and Discussion: The fan-shaped deposit located at the outlet of Bradbury Crater, appears to be centered in a smaller impact crater that formed within Bradbury's crater rim and produced a breach from Bradbury towards the Isidis plains. This local depression is connected to another depression

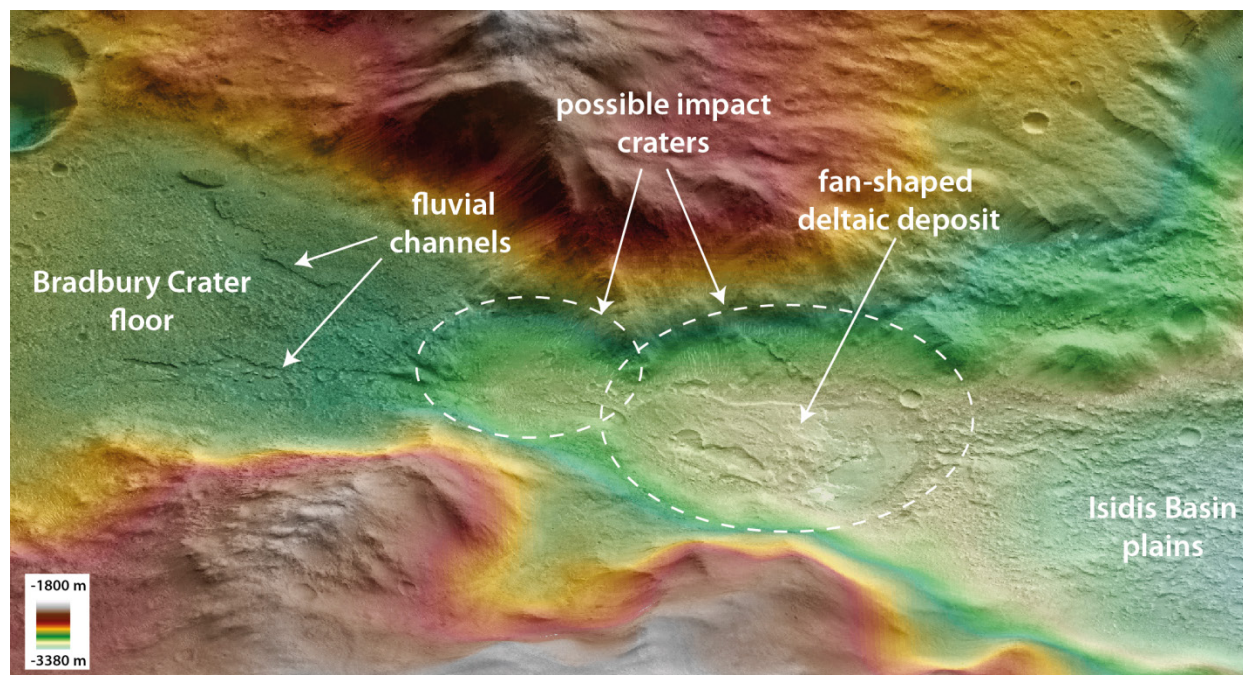


Fig. 1: Perspective view of the fan-shaped deltaic deposit at the Bradbury Crater paleolake outlet bordering Libya Montes and Isidis Planitia. Image width is ~21 km and north is to the right. CTX mosaic over a color-coded HRSC DTM.

located upstream that likewise may represent another impact crater [Fig. 1]. Sediments transported in the two fluvial channels, which drained from Bradbury Crater's interior into these depressions, have been deposited due to decreased flow velocity. Fe/Mg-smectites are detected along the walls of the ancient Libya Montes bedrocks (Fig. 2) and could be a result of Isidis impact-related hydrothermal alteration [cf., 5, 6]. Carbonates intermixed with Fe/Mg-smectites occur at the base of the bedrock unit and show their strongest signature where indicated in yellow (Fig. 2). Carbonate formation may have been driven by the interaction of hydrous CO₂-rich fluids with olivine at the paleolake site. An Al-smectite, consistent with beidellite, is exposed within several layers of the deltaic deposit [cf., 6, 10]. Because beidellite forms at elevated temperatures [6, 10, 11], its presence might either result from alteration in a warm paleolake at this site or it could be an allochthonous sediment deposited here subsequently. Since the strongest beidellite signatures are detected within the foreset and the bottomset layer of the delta [cf., 5, 8], *in situ* alteration in a warm standing body of water is likely, but not certain. If formed shortly after the crater's formation the heat from the crater's impactites could have driven alteration.

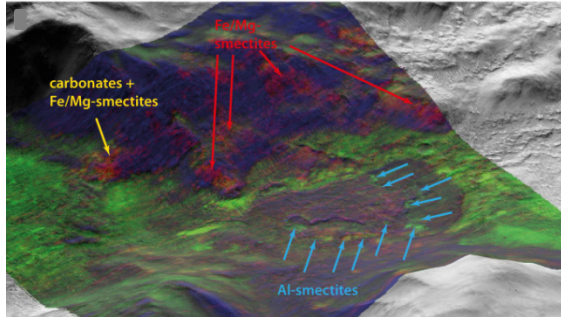


Fig. 2: Location of mineral outcrops at the fan-shaped deltaic deposit as inferred from CRISM IR parameter products. Fe/Mg-smectites are shown in red, carbonates intermixed with Fe/Mg-smectites are shown in yellow and Al-smectites (beidellite in this case) are shown in blue. CRISM spectral parameter map of FRT0000BC0CB (R: D2300, G: OLINDEX, B: LCPINDEX) overlain onto CTX imagery and HRSC topography. North is to the right; image width is ~13.5 km.

Fig. 3 shows the stratigraphic setting of aqueous minerals at the deltaic deposit. Fe/Mg-smectites present in the ancient bedrock are exposed at higher elevations but are stratigraphically lower and older

than the lower lying Al-smectites. These Al-clays could be the result of *in situ* alteration of the lacustrine deposit, or alternatively they might be remnants of former Fe-rich highland clays, which were leached into Al-smectites, transported and deposited here. However, the unique and isolated appearance of the Al-rich deposits more likely supports in-situ formation.

In either scenario, the Al-smectites are significantly younger than the Fe-clays, a stratigraphic situation often observed on Mars [e.g., 12].

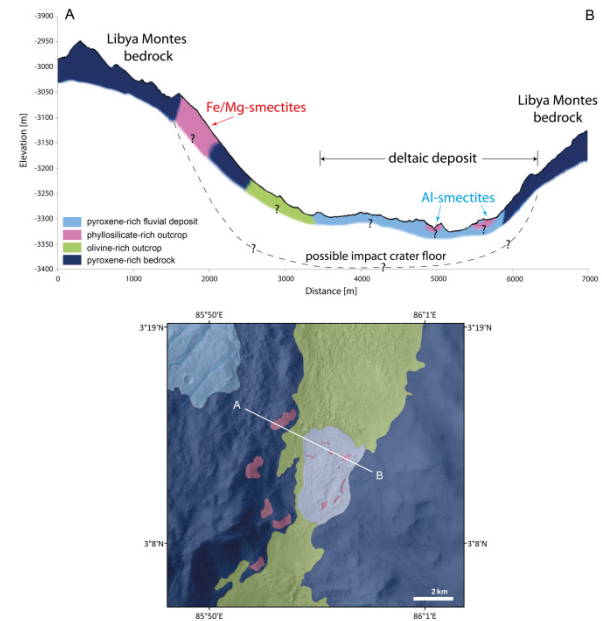


Fig. 3: Top: Geologic cross section through the deltaic deposit at Bradbury Crater from northwest to southeast visualizing the topographic position of hydrated mineral outcrops. Topographic data derived from HiRISE DTM DTEEC_016034_1835_017089_1835_A01. Bottom: CTX image with geologic mapping and profile line.

References: [1] Scott & Tanaka, 1986, *USGS map* # I-1802-A. [2] Crumpler & Tanaka, 2003, *JGR*, 108, doi: 10.1029/2002JE002040. [3] Jaumann et al., 2010, *EPSL*, 294, 272-290 [4] Erkeling et al., 2010, *EPSL*, 294, 291-305. [5] Erkeling et al., 2012, *Icarus*, 219, 393-413. [6] Bishop et al., 2013, *JGR*, 118, 487-513. [7] Tornabene et al., 2008, *JGR*, 113, doi: 10.1029/2007JE002988. [8] Erkeling et al., 2016, *47th LPSC, this issue*. [9] Murchie S. et al., 2009, *JGR*, 114, doi: 10.1029/2009JE003344. [10] Bishop et al., 2011, *Clay & Clay Min.*, 59, 376-397. [11] Guisneau et al., 2007, *Am. Min.*, 92, 1800-1813. [12] Bishop et al., 2013, *PSS* 86, 130-149.